Electronic Supplementary Material (ESI) for RSC Advances.
This journal is © The Royal Society of Chemistry 2016

White Light Emission from Quantum Dot and a UV-visible Emitting Pd-complex on Its Surface

Madhulekha Gogoi* and Arun Chattopadhyay

Department of Chemistry and Centre for Nanotechnology, IIT Guwahati, North Guwahati, PIN- 781039, Assam, India

*E-mail ID: madhulekha@gmail.com

Electronic Supplementary Information

Characterization techniques used

Powder X-ray diffraction was performed with D2 phaser (Bruker). UV-Visible absorption spectra were collected using Lambda 25 spectrometer (Perkin Elmer) and PL spectra by Fluoromax-4 spectrometer (Horriba Scientific). TEM and EDX characterizations were performed with JEM 2100 (JEOL) transmission electron microscope at an accelerating voltage of 200 kV. FTIR spectra were acquired using a Nicolet iS10 (Thermo Scientific) and a Spectrum 2 (Perkin Elmer). Nuclear magnetic resonance (NMR) spectra were collected using a Ascend 600 MHz spectrometer (Bruker) while Electron spin resonance (ESR) spectra by JES-FA 200 spectrometer (JEOL). Time resolved photoluminescence (TRPL) analysis were performed using FSP920 (Eddinburg Instruments) and Quanta Master 30plus (Photon Technologies International). Elemental compositions were estimated by AA240 (Varian) spectrometer. The "go cie" software was used to calculate the chromaticity point in the CIE (1931) diagram. The digital photographs were taken by DSLR D5100 (Nikon). X-ray photoelectron spectra (XPS) of the samples were recorded with a custom built ambient pressure photoelectron spectrometer (APPES) (Prevac, Poland) equipped with a VG Scienta's R3000HP analyzer and MX650 monochromator [S1]. Monochromatic Al Kα X-rays were generated at 200 W and used for measuring the X-ray photoelectron spectrum (XPS) of the above mentioned samples. Base pressure in the analysis chamber was maintained in the range of 5 x 10^{-10} Torr. The energy resolution of the spectrometer was set at 0.7 eV at a pass energy of 50 eV. Binding energy (BE) was calibrated with respect to Au $^4f_{7/2}$ core level at 84.0 eV. Samples were flooded with low energy electrons for efficient charge neutralisation. The electrochemical behavior of the complexes was studied by cyclic voltammetry at 298 K. Cyclic voltammograms (CVs) of complex has been recorded in CH_2Cl_2 solutions containing 0.10 M $[(nBu)_4N]ClO_4$ as supporting electrolyte at a glassy carbon working electrode, a platinum wire counter electrode, and a Ag/AgCl reference electrode. Ferrocene was used as an internal standard, and potentials are referenced versus the ferrocenium/ferrocene couple (Fc^+/Fc).

Measurement of quantum yield (QY)

The measurement of photoluminescence quantum yield (QY) has been carried out for Qdot and QDC by using the comparative method of Williams et al. The equation used is given below (Eq. 1):

$$\emptyset_s = \emptyset_{st}\left(\frac{slope_s}{slope_{st}}\right)\left(\frac{\eta_s^2}{\eta_{st}^2}\right)$$

(1)

Where, ϕ_s and ϕ_{st} are quantum efficiencies of sample and standard, η_s and η_{st} are refractive indices of sample and standard respectively. Here, Tryptophan of quantum efficiency 13% is used as the standard. For determination of the slope, five solutions were prepared for both sample and standard with absorbance below 0.1.

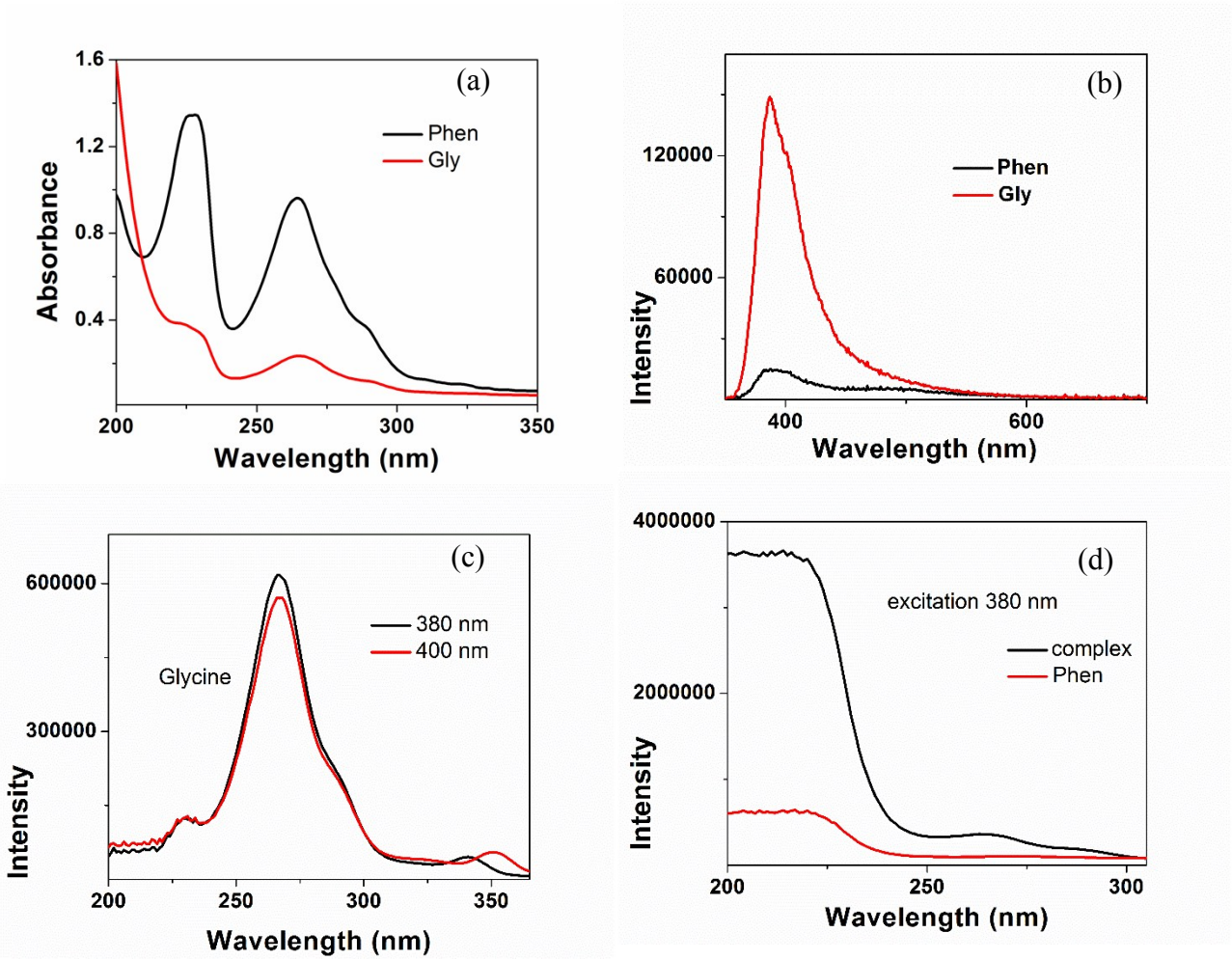

Figure S1. (a) Absorption spectra and (b) emission spectra of glycine and 1,10-phenanthroline ligands (solution in water) with excitation wavelength being set at 270 nm. Excitation spectra of (c) glycine (with emission maxima being set at 380 and 400 nm) and (d) complex and phen ligand (with emission maximum at 380 nm).

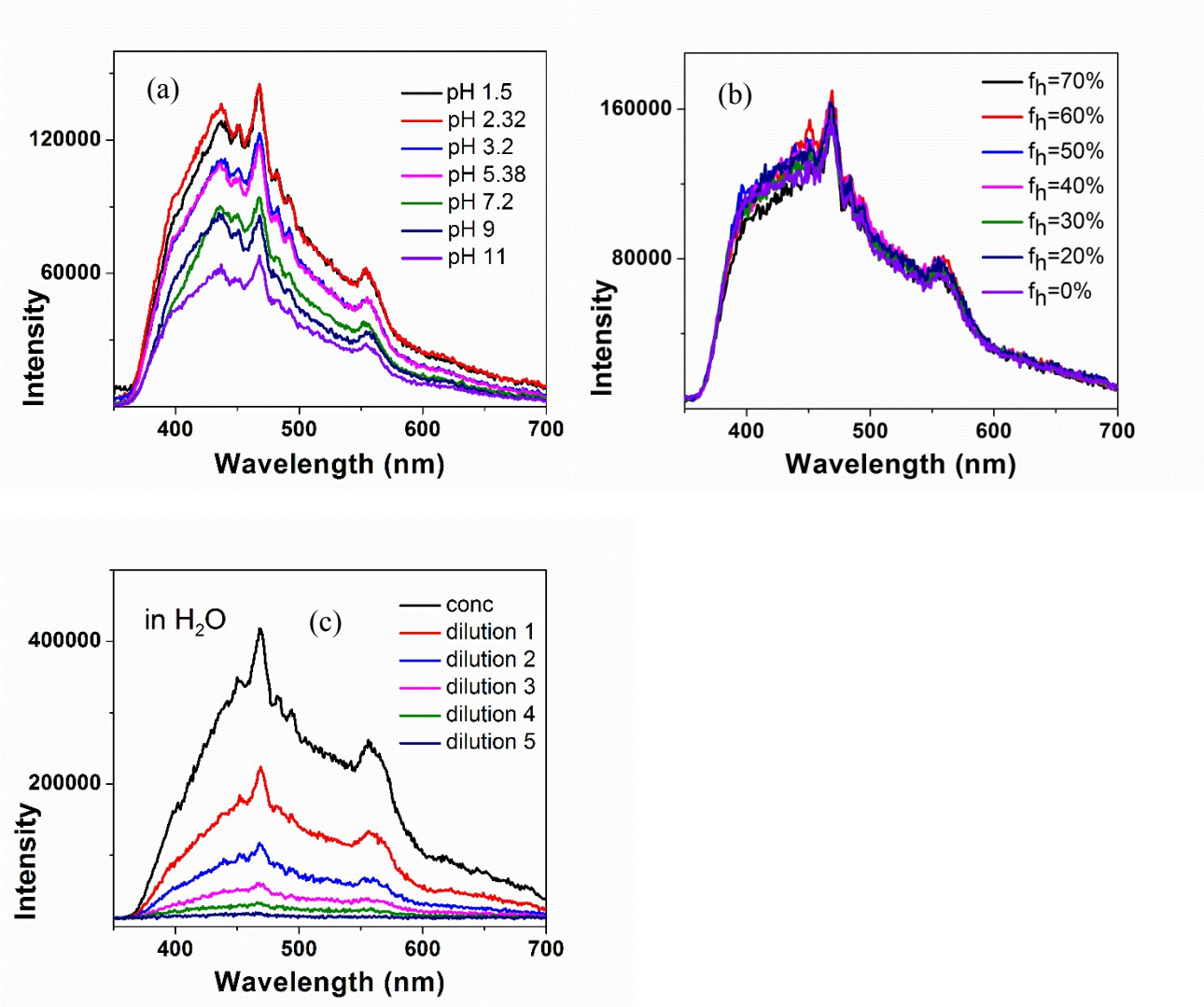

Figure S2. Emission spectra of complex (a) in water recorded at different pH values, (b) in THF/hexane mixed solvents with different fractions of hexane volume (f_h) and (c) in water with dilutions. Excitation wavelength in all studies was 270 nm.

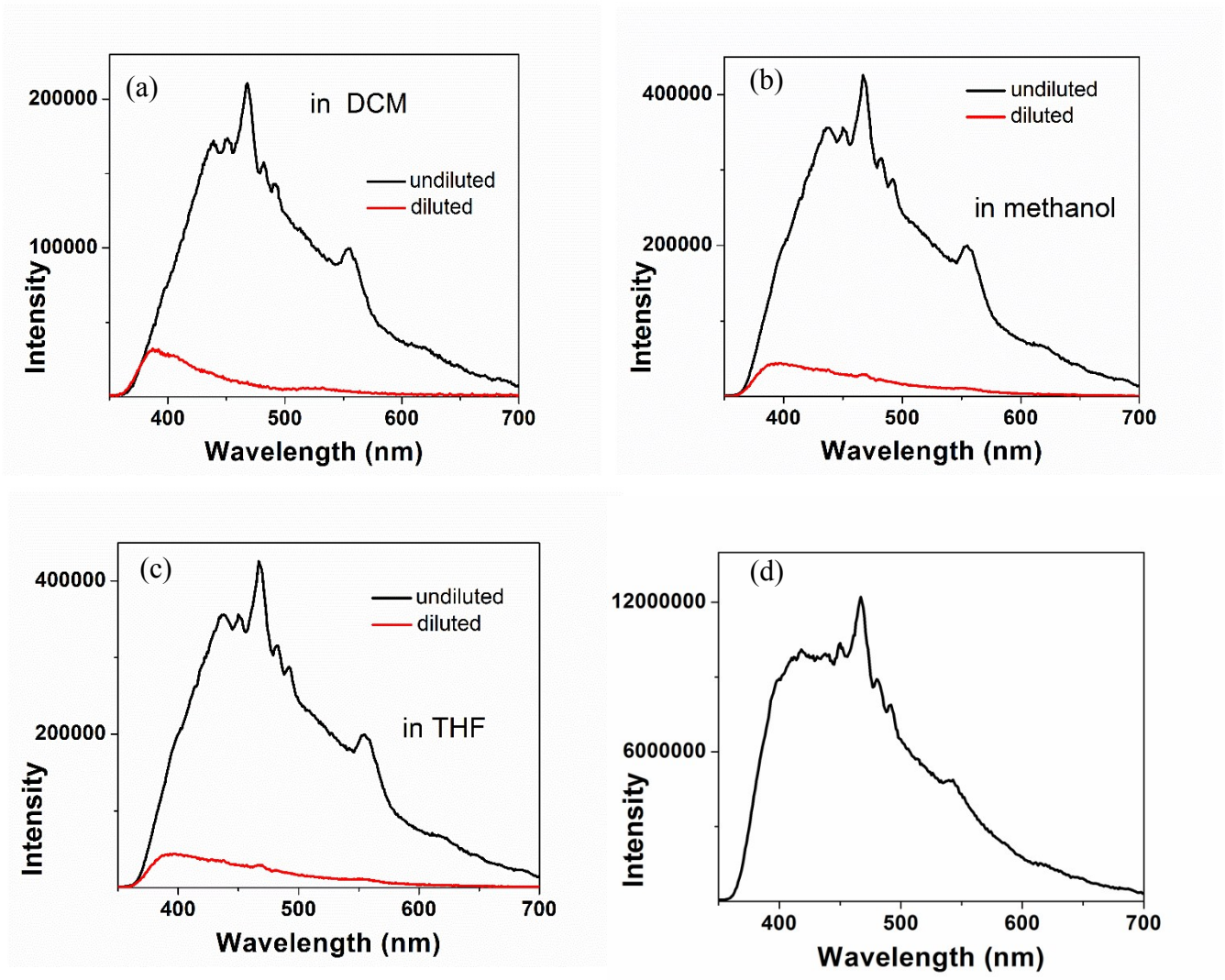

Figure S3. Emission spectra of complex the (as-prepared solution of concentration 0.4 mM and diluted solution with concentration 0.02 mM) in different solvents: (a) dichloromethane, (b) methanol and (c) tetrahydrofuran and (d) solid state fluorescence of the complex. Excitation wavelength was 270 nm.

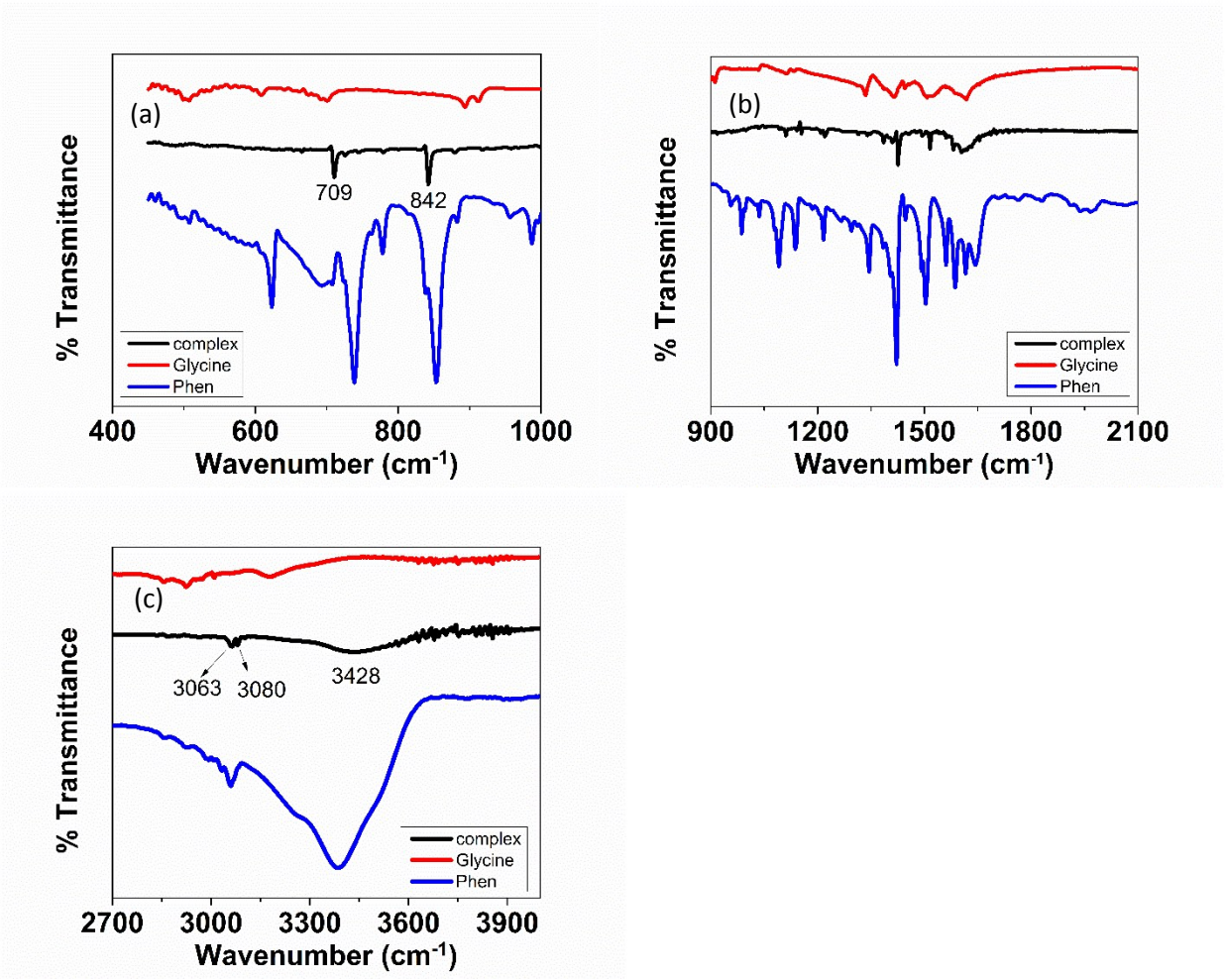

Figure S4. Comparative FTIR spectra of phenanthroline, glycine and the complex.

Table S1. FTIR spectral data comparison among phenanthroline, glycine and the complex (symbol P denotes present data).

Wavenumber (cm^{-1})	**Functional groups**	**Phenanthroline**	**Glycine**	**Complex**
3428	$NH_{stretch}$	P (3383) broad		P (broad)
3081	$NH^{3+}_{antisymm}$		P (3175, zwitterion)	P
3063	NH^{3+}_{symm}	P	P (3075, zwitterion)	P
2927	$CH_{2\ stretch}$	P	P	P
2854	$CH_{2\ stretch}$	P	P	P
1640	quadruple for ring frequencies	P		
1618	quadruple for ring frequencies	P	P	P (1600)
1584	quadruple for ring frequencies	P	P	
1562	quadruple for ring frequencies	P		
1516	$NH^{3+}_{bending}$ /COO- antisymm for zwitterion C=C $_{stretch}$	P (1500)	P (broad)	P
1446	$CH_{2\ deform}$	P	P	
1420	COO- symm for	P	P	P (1424)

	zwitterion)			
1383	vibrational stretch of COO-	P	P	P
1343	$CH_{2\ deform}$ / C-N $_{stretch}$ (aromatic)	P	P (1338)	P (1341)
1219	In plane H deformation motion	P		P
1206	In plane H deformation motion	P		P
1136	In plane H deformation motion	P	P	P (1141)
1110	C-N $_{stretch}$ (aliphatic)		P	P
1052	C-O stretching			P
912	N-H $_{wag}$		P	P (920)
893	CN^+/CC^+		P	P
879	Out of plane motion of ring H	P		P
853	Out of plane motion of ring H	P		P (842) decreased sharply
776	Out of plane motion of ring H	P		P
738	Out of plane motion of ring H	P		P (747) decreased sharply
709	Out of plane motion of ring H	P	P (711)	P (711)
666	In plane motion of COO- group adsorbed onto surface			P
607	In plane motion of COO- group adsorbed onto surface		P	

514	In plane motion of COO- group adsorbed onto surface	P	P	

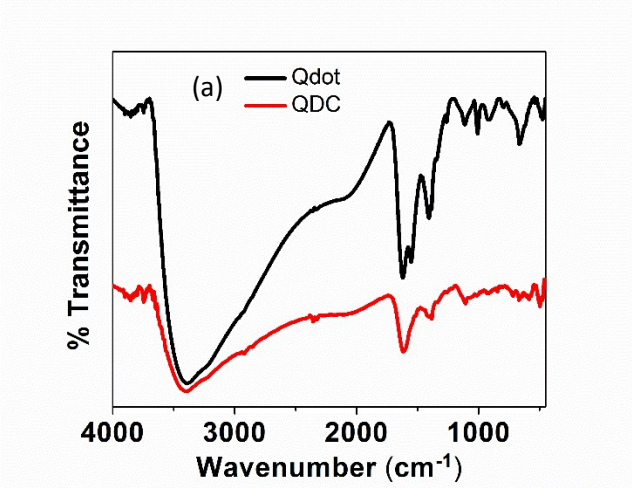

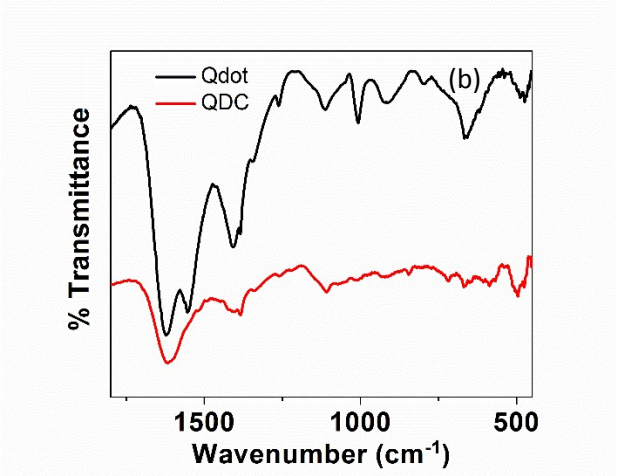
Qdot
QDC
(b)
% Transmittance
1500
1000
500
Wavenumber (cm-1)

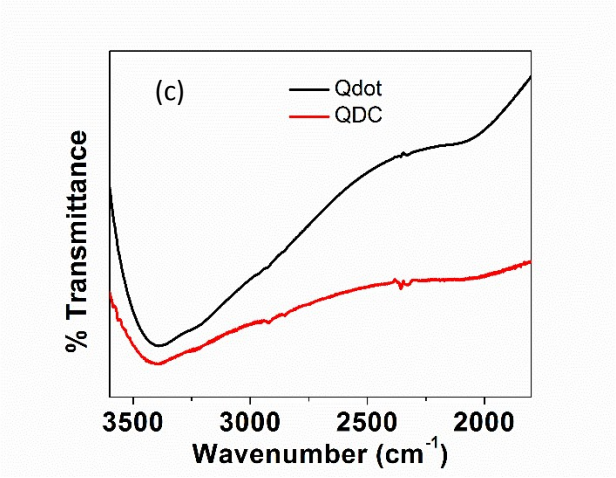
(c)
Qdot
QDC
% Transmittance
3500
3000
2500
2000
Wavenumber (cm-1)

Figure S5. Comparative FTIR spectra of Qdot and QDC.

Table S2. FTIR spectral data comparison between Qdot and QDC. Here P denotes present data.

Wavenumber (cm^{-1})	**Functional groups**	**Qdot**	**QDC**
472	M-N stretching		P
507	In plane motion of COO- group adsorbed onto surface		P
661	C-H bending	P	
667	In plane motion of COO- group adsorbed onto surface		P
720	Out of plane motion of ring H		P
796	C-H out of plane deformation	P	
844	Out of plane motion of ring H		P
796	C-H out of plane deformation	P	
1007	C-H in plane deformation	P	
1114	-C-O-M / C-H in plane deformation	P	P (observed at 1105 cm^{-1})
1260	C-H in plane deformation	P	
1385	vibrational stretch of COO-	P	P (weak)
1406	symmetric stretch of COO-	P	P (weak)
1555	antisymmetric stretch of COO-	P	
1616 (broad)	quadruple for ring frequencies		P
1620	O-H bending vibration	P	
2851	CH_2 antisymmetric stretching		P

2920	CH_2 symmetric stretching		P
3385	O-H stretching vibration / N-H stretching vibration	P	P

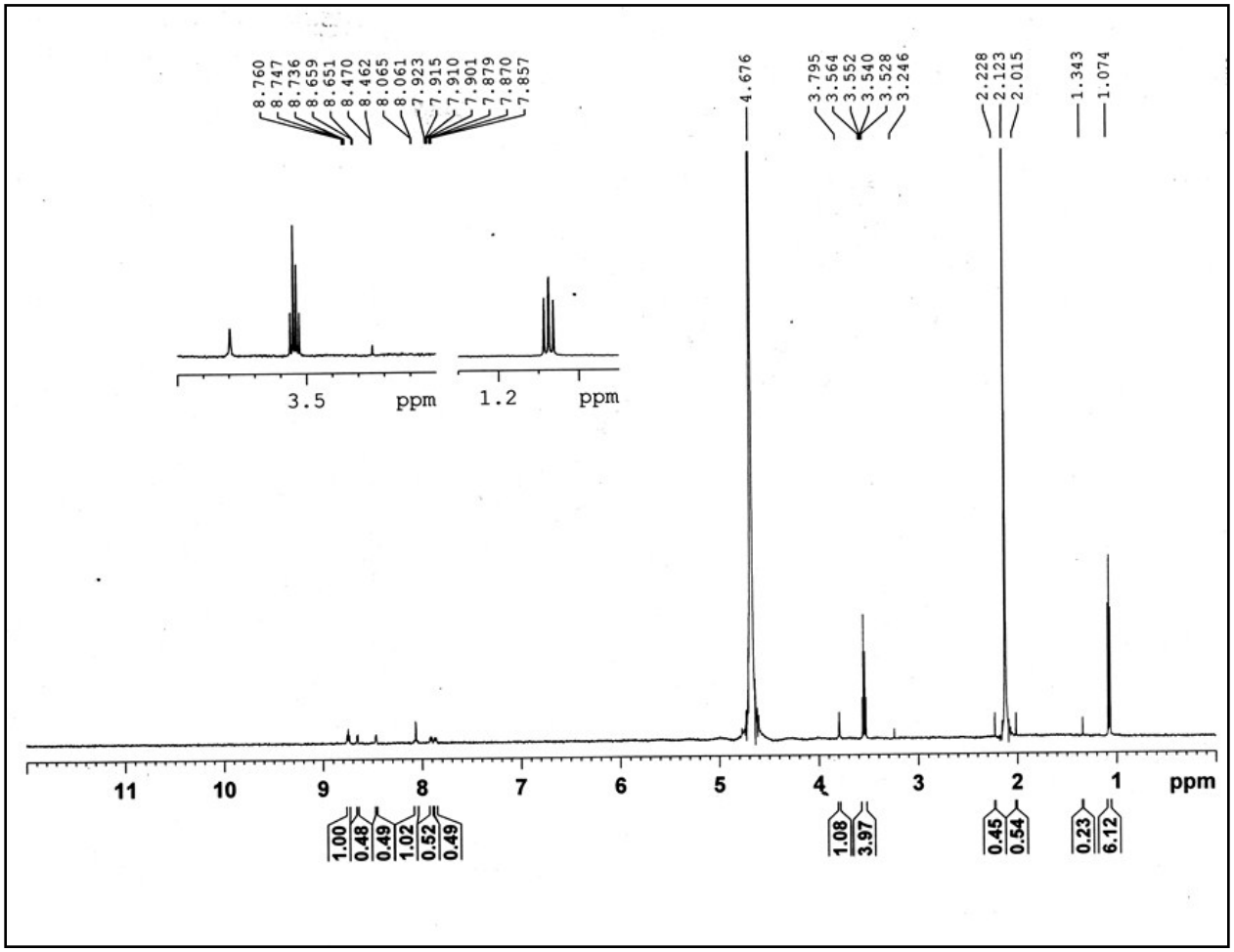

Figure S6. H^1-NMR spectra of the complex.

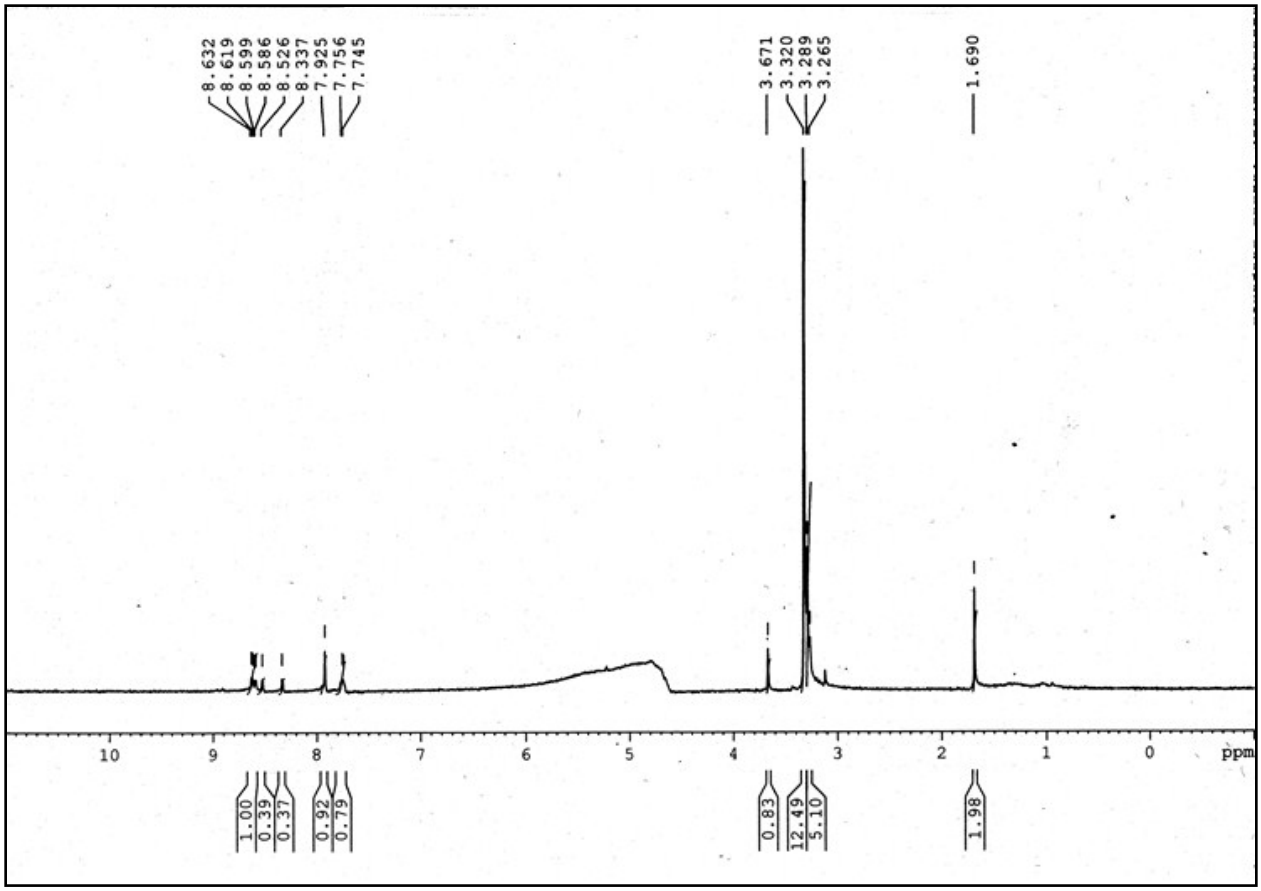

Figure S7. H^1-NMR spectra of the QDC.

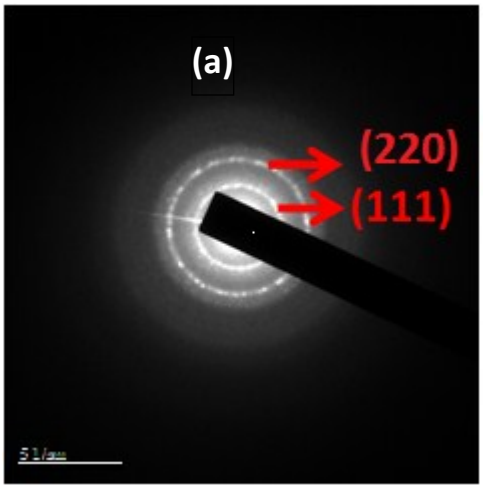
(a)
(220)
(111)

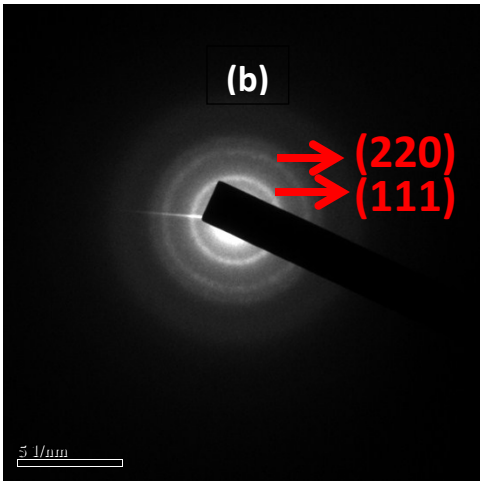
(b)
(220)
(111)

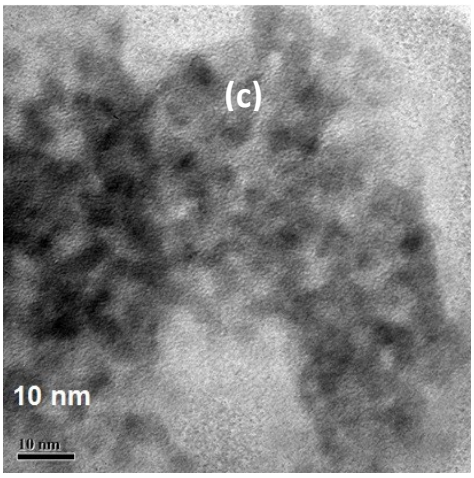
(c)
10 nm

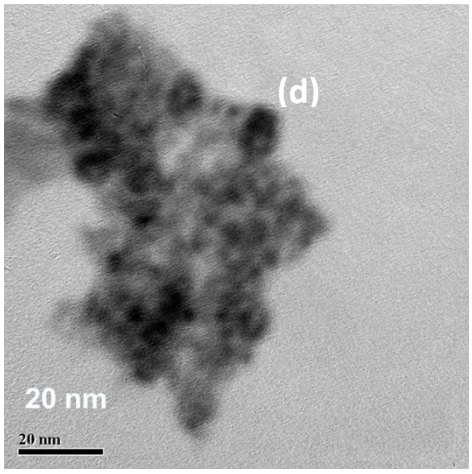
(d)
20 nm

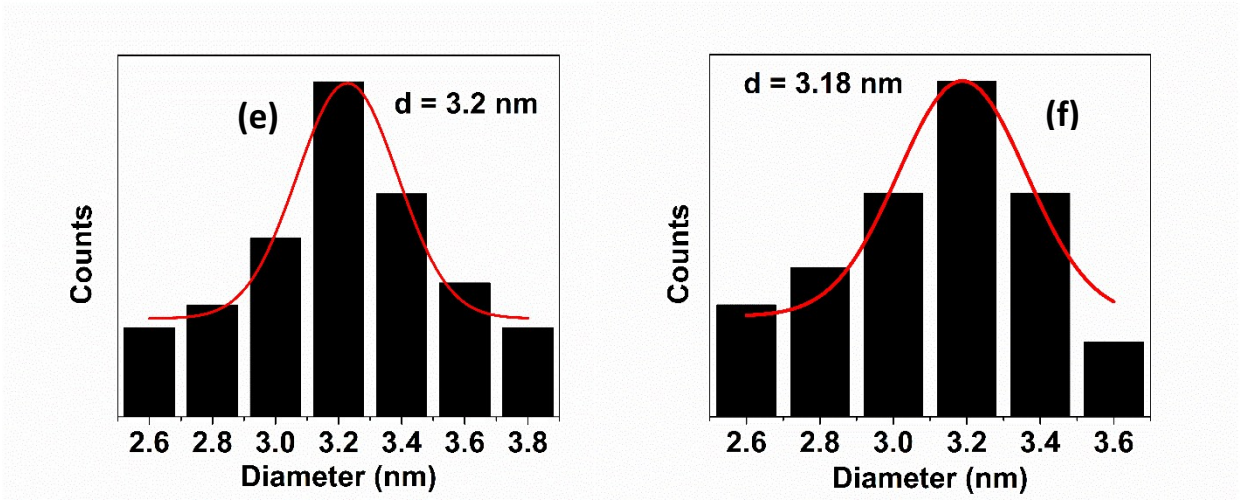
(e)
d = 3.2 nm
Counts
2.6 2.8 3.0 3.2 3.4 3.6 3.8
Diameter (nm)
d = 3.18 nm
(f)
Counts
2.6 2.8 3.0 3.2 3.4 3.6
Diameter (nm)

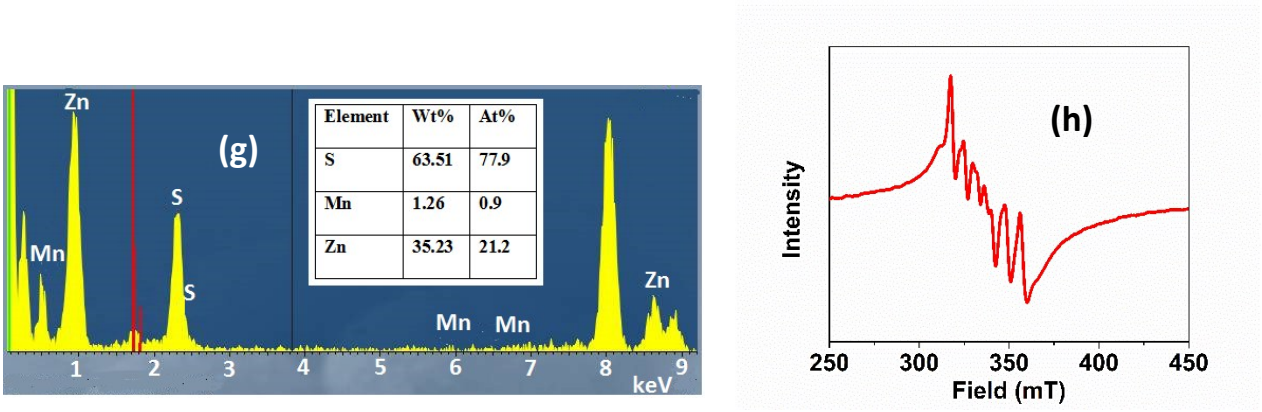

Figure S8. Selected area diffraction pattern (SAED) of (a) Qdot and (b) QDC. TEM images of (c) Qdot and (d) QDC. Particle size distribution plot of (e) Qdot and (f) QDC. Particle sizes were calculated from the TEM images. (g) EDS spectrum of Qdot and (h) ESR spectrum of QDC.

Table S3. Compositional analysis of Qdot.

Element	Atomic % EDS	Conc (ppm) AAS	Ratio
Zn	21.2	3.98	0.04
Mn	0.9	0.16	0.04

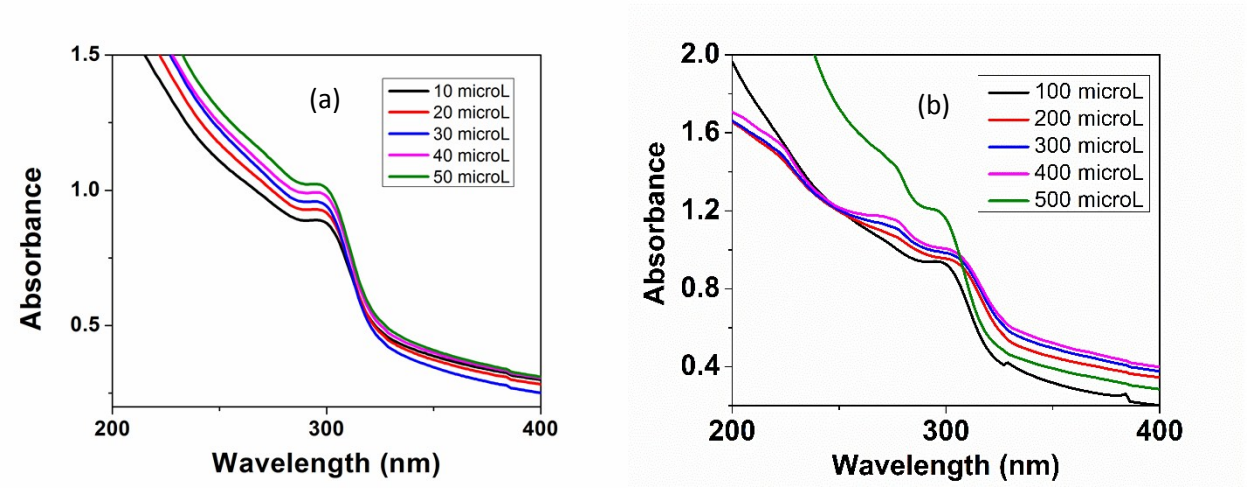

Figure S9. UV-Visible absorption spectra of QDC formed by adding different volumes of complex solutions (0.1 μM with respect to Pd^{2+} ion).

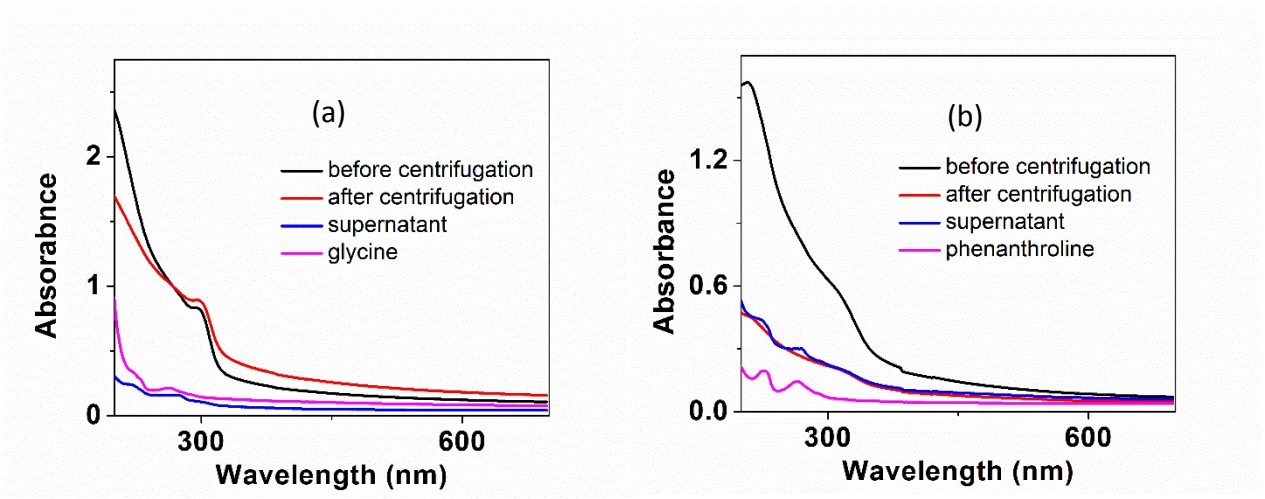

Figure S10. UV-Visible absorption spectra of (a) Qdot solution treated with glycine solution (13.3 mM) and (b) Qdot solution treated with phenanthroline solution (4.4 mM).

Table S4. Absorption peaks observed from Figure S7.

Sample name	Peak positions in the absorption spectra
Qdot	300 nm
QDC	300 nm, 272 nm and 220 nm
Complex	272 nm and 220 nm
Glycine	268 nm and 224 nm
Phenanthroline	265 nm and 227 nm

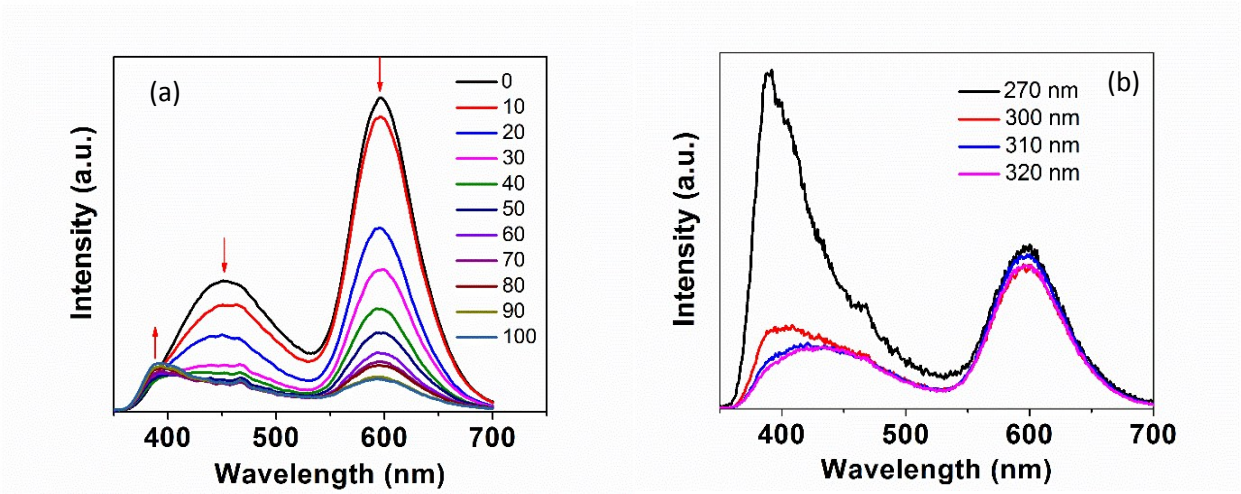

Figure S11. Fluorescence spectra of (a) QDC obtained by addition of different volumes (in µL) of complex solution (0.1 µM) at excitation 300 nm and (b) QDC excited by different wavelengths.

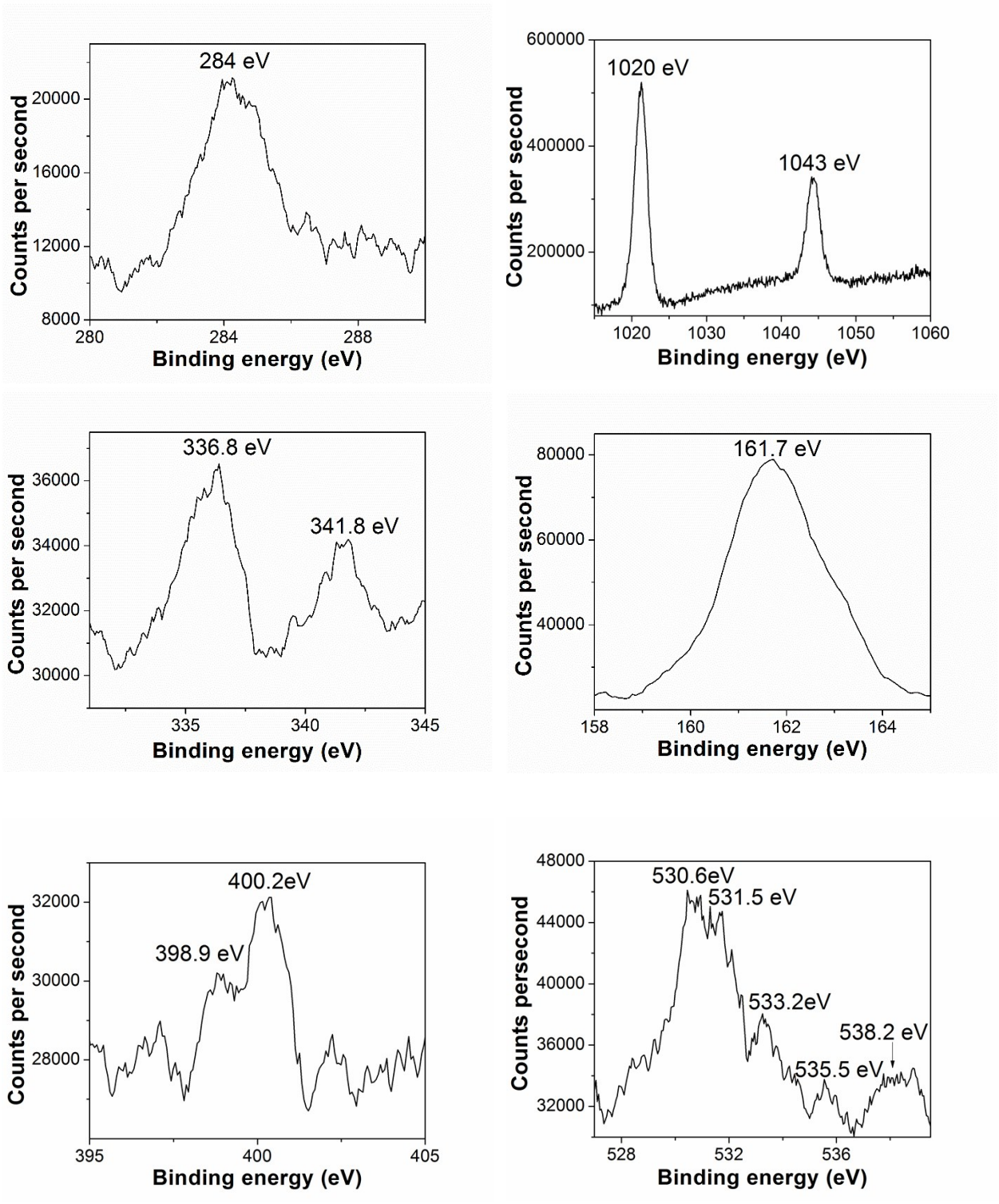

Figure S12. XPS spectra of (a) C 1s, (b) Zn 2p, (c) Pd 3d, (d) S 2p, (e) N 1s and (f) O 1s peak of QDC.

In the XPS spectra of C 1s (Fig. S12(a)), the peak at 284 eV corresponds to aliphatic carbon (C–C) of glycine, phenanthroline ligands [S2]. The Zn 2p spectra (Fig. S12(b)) has two peaks at 1020 eV and 1044 eV. These two peaks are attributed to the presence of Zn^{2+} [S3]. The Pd 3d spectra (Fig. S12(c)) shows the presence of peaks at 336.8 eV and 341.8 eV which correspond to Pd $3d_{3/2}$ and $3d_{5/2}$ electrons and proves the presence of Pd^{2+} only [S4]. In the S 2p spectra (Fig. S12(d)), the only peak at 161.7 eV corresponding to bound thiols has been observed [S5]. N1s XPS spectra (Fig. S12(e)) consists of two peaks: at 400.2 eV corresponding to zwitterionic NH_3^+ of glycine [S6] and at 398.9 eV corresponding to metal-N [S7] which may be of phenanthroline bonded to Pd. The peaks observed in the XPS spectra of O1s (Fig. S12(f)) are assigned as: 530.6 eV to O bound to metal, 531.5 eV to –OH [S5], 533.2 eV to C=O [S8], 535.5 eV to satellite [S9] and 538.2 eV to bridging O atom [S10].

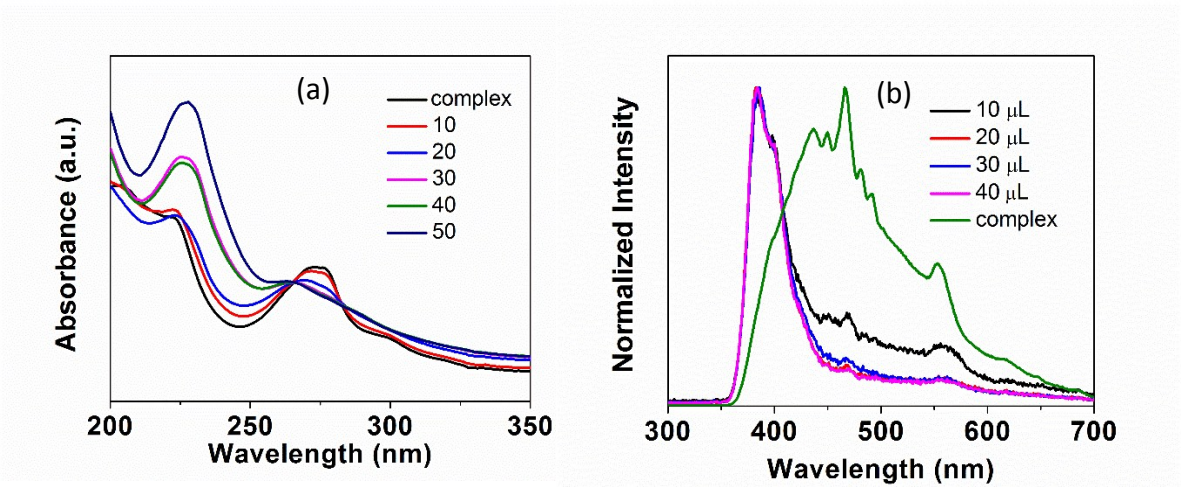

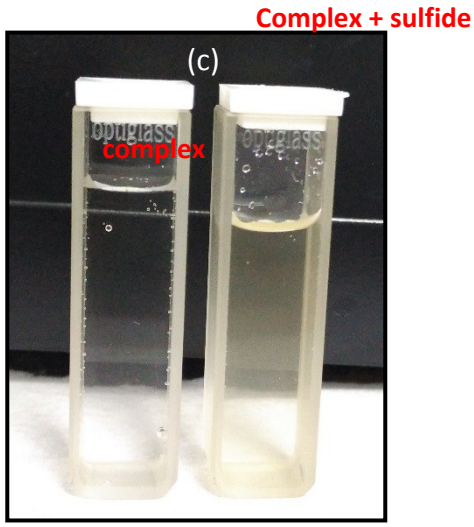

Figure S13. (a) UV-Visible absorption spectra, (b) photoluminescence spectra (excitation 270 nm) of the complex added with different volumes of Na_2S solution (in μL) and (c) Digital photographs of complex solution before and after addition of sulfide solution.

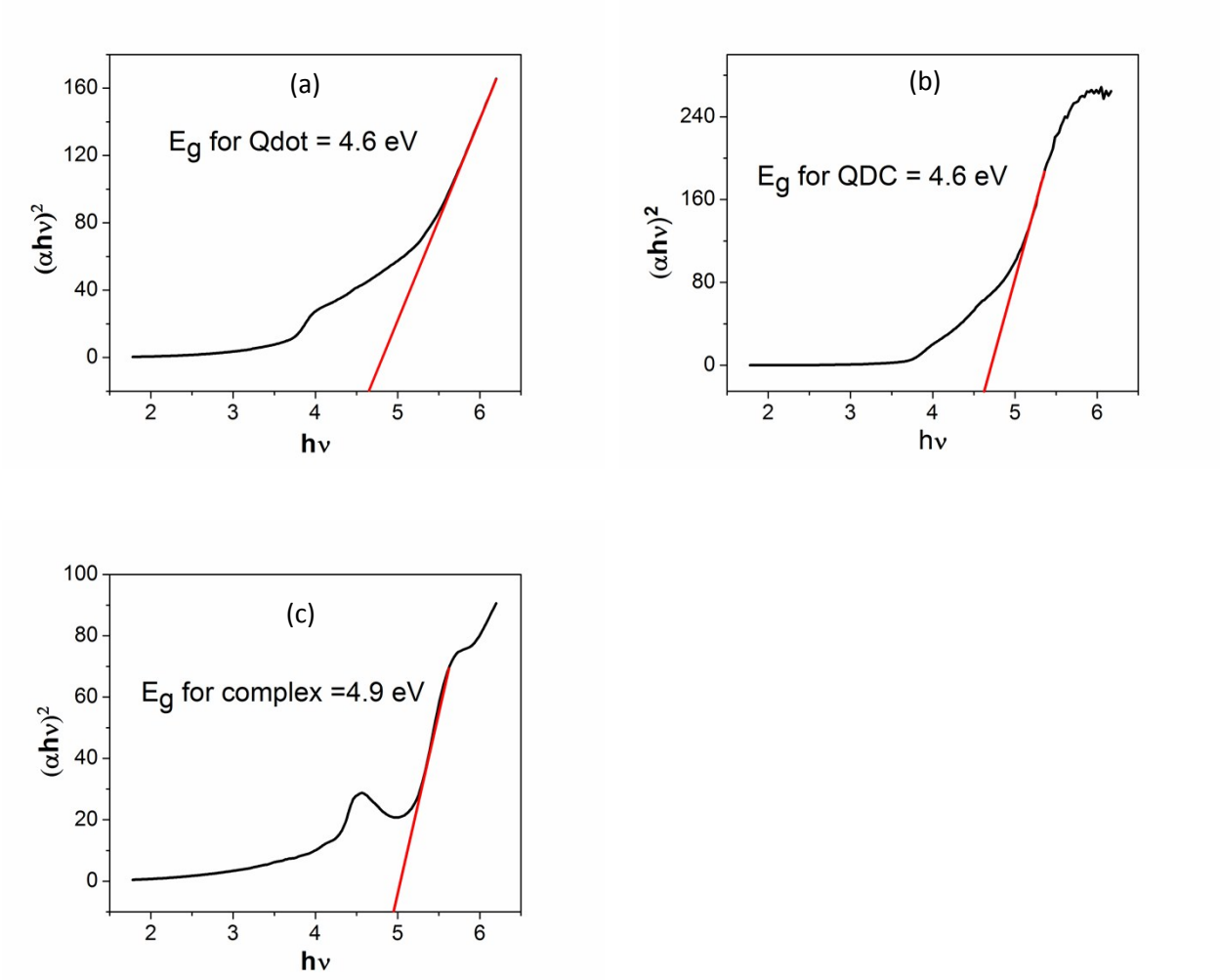

Figure S14. Tauc's plot of (a) Qdot, (b) QDC and (c) complex.

Table S5. Fluorescence decay parameters of Qdot and QDC monitored at 450 nm (excitation 290 nm LED)

Sample	α_1(%)	τ_1 (ns)	α_2(%)	τ_2(ns)	τ_{av}(ns)	χ^2
Qdot	45	2.1	27.98	27.98	26.46	1.07
QDC	32.26	1.45	67.74	8.9	7.66	0.964

Table S6. Phosphorescence decay parameters of Qdot, QDC and complex monitored at 597 nm (excitation 320 nm), 390 nm (excitation 270 nm) and 390 nm (excitation 270 nm) respectively

Sample	α_1(%)	τ_1 (μs)	α_2(%)	τ_2(μs)	α_3(%)	τ_3(μs)	τ_{av}	χ^2
complex	99.99	5.1	-0.65	6.7	0.001	9.7	5	1.1
QDC	-0.005	3.5	99.99	1.7	1.2×10^{-11}	8.9	1.69	1.2
Qdot	0.126	785	16055	6	-	-	6.79	0.99

References:

[S1] K. Roy, C. P. Vinod and C. S. Gopinath, J. Phys. Chem. C 117, 4717, 2013.

[S2] B. A. de Angelis, C. Rizzo, S. Contarini and S. P. Howlett, Appl. Surface Sci. 51, 177-183, 1991.

[S3] P. Sakthivel, S. Muthukumaran and M. Ashokkumar, J. Mater. Sci.: Mater. Electron. 26, 1533-1542, 2015.

[S4] V. N. Mikhaylov, V. N. Sorokoumov, K. A. Korvinson, A. S. Novikov and I. A. Balova, Organometallics 35, 1684-1697, 2016.

[S5] M. Gogoi, P. Deb, G. Vasan, P. Keil and A. Erbe, Appl. Surface Sci. 258, 9685-9691, 2012.

[S6] M. Z. Atassi and E. Appella, Methods in Protein Structure Analysis, Springer Science and Business Media 2013, pp. 256.

[S7] S. Seal, Chemical Mechanical Planarization VI: Proceedings of the International Symposium, The Electrochemical Society2003, pp. 58.

[S8] J. L. Droulas, T. M. Duc and Y. Jugnet, The Empty The Thin Films, Supplement no. 258, 39-41, 1991.

[S9] C. Mustin, P. D. Donato and R. Benoit, Appl. Surface Sci. 68, 147-158, 1993.

[S10] H. Goretzki, H. U. Chun, M. Summet and R. Bruckner, J. Non-crystalline Solids, 42, 49-60, 1980.